AD-A115 194 ROCHESTER UNIV NY DEPT OF CHEMISTRY F/G 20/5
LASER-INDUCED GAS-PHASE AND SURFACE RATE PROCESSES: ELECTRONIC --ETC(U)
MAY 82 T F GEORGE, K LAN, M HUTCHINSON N00014-80-C-0472
UNCLASSIFIED TR-19 NL

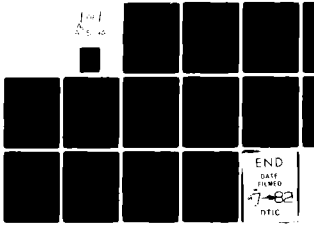

END
DATE FILMED
7-82
DTIC

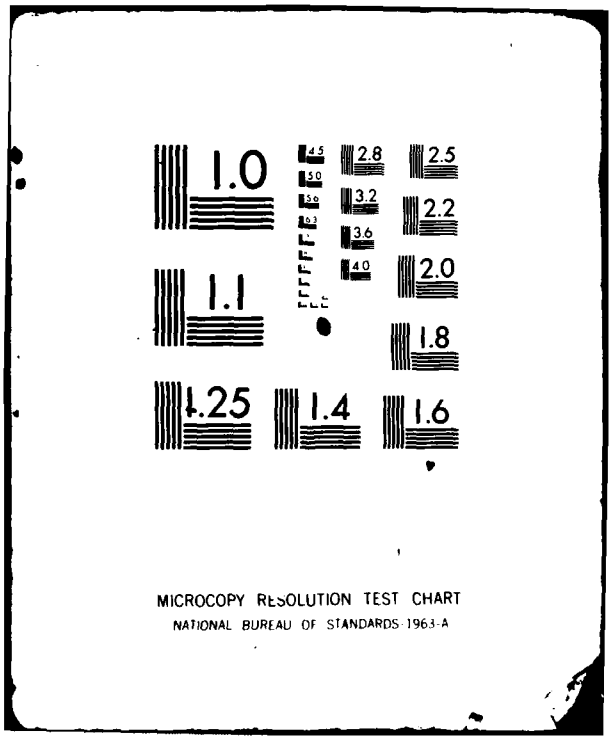
1.0
1.1
1.25
1.4
1.6
1.8
2.0
2.2
2.5
2.8
3.2
3.6
4.0
4.5
5.0
5.6
6.3
MICROCOPY RESOLUTION TEST CHART
NATIONAL BUREAU OF STANDARDS-1963-A

OFFICE OF NAVAL RESEARCH

Contract N00014-80-C-0472

Task No. NR 056-749

TECHNICAL REPORT No. 19

Laser-Induced Gas-Phase and Surface Rate Processes: Electronic Excitations and Bound-Continuum Interactions

by

Thomas F. George, Kai-Shue Lam,
Michael Hutchinson and William C. Murphy

Prepared for Publication

in

Advances in Laser Spectroscopy, Vol. 2, ed. by
B. A. Garetz and J. R. Lombardi (Heyden, Philadelphia, 1982)

University of Rochester
Department of Chemistry
Rochester, New York 14627

May, 1982

Unclassified

SECURITY CLASSIFICATION OF THIS PAGE (When Data Entered)

REPORT DOCUMENTATION PAGE	READ INSTRUCTIONS BEFORE COMPLETING FORM
1. REPORT NUMBER: 19	2. GOVT ACCESSION NO.: AD-A115198
3. RECIPIENT'S CATALOG NUMBER:	
4. TITLE (and Subtitle): Laser-Induced Gas-Phase and Surface Rate Processes: Electronic Excitations and Bound-Continuum Interactions	5. TYPE OF REPORT & PERIOD COVERED: Interim Technical Report
	6. PERFORMING ORG. REPORT NUMBER:
7. AUTHOR(s): Thomas F. George, Kai-Shue Lam, Michael Hutchinson and William C. Murphy	8. CONTRACT OR GRANT NUMBER(s): N00014-80-C-0472
9. PERFORMING ORGANIZATION NAME AND ADDRESS: University of Rochester, Department of Chemistry, Rochester, New York 14627	10. PROGRAM ELEMENT, PROJECT, TASK AREA & WORK UNIT NUMBERS: NR 056-749
11. CONTROLLING OFFICE NAME AND ADDRESS: Office of Naval Research, Chemistry Program Code 472, Arlington, Virginia 22217	12. REPORT DATE: May 1982
	13. NUMBER OF PAGES: 25
14. MONITORING AGENCY NAME & ADDRESS(if different from Controlling Office)	15. SECURITY CLASS. (of this report): Unclassified
	15a. DECLASSIFICATION/DOWNGRADING SCHEDULE:

16. DISTRIBUTION STATEMENT (of this Report)

This document has been approved for public release and sale; its distribution is unlimited.

17. DISTRIBUTION STATEMENT (of the abstract entered in Block 20, if different from Report)

18. SUPPLEMENTARY NOTES

Prepared for publication in Advances in Laser Spectroscopy, Vol. 2, ed. by B. A. Garetz and J. R. Lombardi (Heyden, Philadelphia, 1982).

19. KEY WORDS (Continue on reverse side if necessary and identify by block number)

LASER-INDUCED RATE PROCESSES	PENNING AND ASSOCIATIVE IONIZATION
ELECTRONIC EXCITATIONS	SEMICONDUCTOR SURFACE STATES
ATOM-ATOM COLLISIONS	BAND GAP
MULTIPHOTON RESONANCES	INCREASED SURFACE CHARGE
LASER-ENHANCED CURVE SWITCHING	LASER-ENHANCED DESORPTION

20. ABSTRACT (Continue on reverse side if necessary and identify by block number) Two different types of laser-induced gas-phase rate processes are studied theoretically: collisional ionization and multiphoton resonances in atom-atom scattering. The first involves the coupling between bound and continuum electronic states, and the second between bound and continuum vibrational states. In connection with surface processes, the use of a laser to excite electrons from the valence band to surface states of a semiconductor and the resulting effect on an adspecies is explored.

DD FORM 1 JAN 73 1473 EDITION OF 1 NOV 65 IS OBSOLETE S/N 0102-LF-014-6601

Unclassified

SECURITY CLASSIFICATION OF THIS PAGE (When Data Entered)

LASER-INDUCED GAS-PHASE AND SURFACE RATE PROCESSES: ELECTRONIC EXCITATIONS AND BOUND-CONTINUUM INTERACTIONS

Thomas F. George, Kai-Shue Lam, Michael Hutchinson
and William C. Murphy
Department of Chemistry
University of Rochester
Rochester, New York 14627

Two different types of laser-induced gas-phase rate processes are studied theoretically: collisional ionization and multiphoton resonances in atom-atom scattering. The first involves the coupling between bound and continuum electronic states, and the second between bound and continuum vibrational states. In connection with surface processes, the use of a laser to excite electrons from the valence band to surface states of a semiconductor and the resulting effect on an adspecies is explored.

to appear in Advances in Laser Spectroscopy, Vol. 2, ed. by B. A. Garetz and J. R. Lombardi (Heyden, Philadelphia, 1982).

I. Introduction

Theoretical studies are presented for two different types of laser-induced gas-phase rate processes. The first (Sec. II. A) is collisional ionization, where the radiation couples bound and continuum electronic states of two colliding atoms. The theory relies on classical mechanics for a description of the nuclear motion, but treats the electronic degrees of freedom quantum mechanically. The second process (Sec. II. B) is multiphoton resonances in atom-atom scattering, where laser radiation induces transitions to quasi-bound rovibrational states during the course of the collision. The collision process is considered in the presence of two simultaneous lasers (intensity less than 1 kW/cm^2), with all molecular degrees of freedom treated quantum mechanically. The possibility of enhanced curve switching by this process is investigated. Finally, in Sec. III, the use of laser radiation to excite electrons from the valence band to surface states of a semiconductor is considered. This can lead to increased charge in the surface region and hence a strong Coulombic interaction with an adspecies, which is calculated for a model system.

II. Gas-Phase Processes

A. Collisional Ionization

There are really two problems, the structural and the dynamical. The structural part is concerned with suitable choices of electronic basis functions, potential surfaces, coupling matrix elements and the like. These are massive problems which we are not equipped to address. Our attention will be devoted to the dynamical part ——

the solution of the equations of motion describing ionization events, given the raw structural ingredients.

The simplest situation one can imagine —— and we will be working in this framework —— is an atom-atom collision involving the ejection of a single electron in which the different partial wave events are decoupled. Let us just look at the ℓ-th partial wave. The radial wave function, $\underset{\sim}{\psi}^{(\ell)}(R)$ (R = internuclear distance), can then be regarded as a vector with the components $(\psi_d^{(\ell)}(R), \psi_\varepsilon^{(\ell)}(R))$. d stands for the initial discrete channel and ε for a continuum of channels, one for each possible energy of the emitted electron. It is apparent that $0 < \varepsilon < \infty$. Now the dynamicist decides on what electronic basis to work with —— let us say the one in which motional or nonadiabatic couplings between the different channels are banned, usually called the diabatic representation. The structuralist then hands him the corresponding set of 'matrix elements', consisting of the discrete and ionization threshold potential curves, $W_2(R)$ and $W_1(R)$ respectively, and the bound continuum couplings, $V_\varepsilon(R)$. If for the moment we regard ε as a denumerably infinite descretized set, the time-independent Schrödinger equation can be cast in the form

$$\left\{ \nabla_R^2 - \frac{2\mu}{\hbar^2} \left(\begin{array}{cccc} W_2 & V_{\varepsilon_1} & V_{\varepsilon_2} & \cdots \\ V_{\varepsilon_1} & W_1+\varepsilon_1 & & \bigcirc \\ V_{\varepsilon_2} & & W_1+\varepsilon_2 & \\ \vdots & \bigcirc & & \ddots \end{array} \right) - \frac{\ell(\ell+1)}{R^2} + k^2 \right\} \begin{bmatrix} \psi_d^{(\ell)} \\ \psi_{\varepsilon_1}^{(\ell)} \\ \psi_{\varepsilon_2}^{(\ell)} \\ \vdots \end{bmatrix} = 0, \qquad (1)$$

an infinite set of coupled differential equations. We note here that Eq. (1) is not only good for the description of ionization. It can also be looked at under the guise of the problem of collisionally-induced light emission. Eq. (1) is not easy to solve in general. Various ways have been devised to get around it. First, if one is not interested in a particular ε channel but only in the total decay rate from the d channel, a complex potential $W = W_2 + iV_\varepsilon$ (non-Hermitian and hence non-energy conserving) can be introduced to describe the decay [1]. One then just solves

$$\left(\nabla_R^2 - \frac{2\mu}{\hbar^2} W - \frac{\ell(\ell+1)}{R^2} + k^2\right) \psi_d^{(\ell)} = 0 \ . \qquad (2)$$

Alternatively, one can introduce a specific discretization scheme and pick out only the ε of interest to do the problem, or at most a few of the nearby channels, arguing that, on the basis of the Franck-Condon principle, only *nuclear energy conserving* ionization events are significant: In this case $W_1+\varepsilon$ is required to be equal to, or at least approximately equal to W_2. When one takes this approximation seriously, the two-state coupled-channels discretization procedure [2] results, in which one just solves

$$\left\{\nabla_R^2 - \frac{2\mu}{\hbar^2}\begin{pmatrix} W_2 & V_\varepsilon \\ V_\varepsilon & W_1+\varepsilon \end{pmatrix} - \frac{\ell(\ell+1)}{R^2} + k^2\right\}\begin{pmatrix} \psi_d^{(\ell)} \\ \psi_\varepsilon^{(\ell)} \end{pmatrix} = 0 \ . \qquad (3)$$

Variations of this theme involve the inclusion of a few other nearby channels. The above treatments are within the framework of 'exact' quantum mechanics. They have been amply worked over and demonstrated to have been successful to a certain extent. We will not pursue them further here.

That quantum mechanics furnishes the ultimately correct approach to these problems is of course not disputed. It is not even claimed that the so-called semiclassical methods are necessarily more labor saving. Nevertheless, it is interesting to see what classical mechanics can do for us, simply because, in some sense, it is more intuitive. In certain cases it is much easier to think of dynamics in terms of billiard balls moving on potential surfaces rather than colliding wave packets with probabilities of ending up in different channels. But the question of exactly how far one can push classical mechanics in molecular dynamics has never really been settled, nor can we pretend to be able to supply an answer here.

The central idea of semiclassical methods involves the notion of classical trajectories (R as a definite function of t), foregoing the notion of deterministic trajectories given a fixed set of initial conditions. This effectively means that the dynamics in different channels can interfere; but in each it is governed by a certain R(t). The interference leads to quantum mechanical results otherwise not obtainable from straight classical mechanics.

We will now apply these ideas to the problem of collisional ionization [3]. First, instead of Eq. (1), we can use the time-dependent Schrödinger equation, since R is already regarded as a function of t. In so doing, the second-order coupled differential equations (in R) will become first-order ones (in t). Then comes a re-examination of the choice of basis. Do we still want to work with the one used in Eq. (1)? We can, of course, but we can also, by a transformation of basis, turn what is apparently a problem in Eq. (1) (that of the infinitely coupled nature of the equations) into

an advantage. We can use a basis set, characterized only by ε and diagonal in ε, make ε continuous, and turn Eq. (1) into a simple differential-integral equation. This is sometimes called a Lee-model approach. Thus

$$\begin{pmatrix} \cdot & & \\ & \underset{\approx}{D}^{(R)}_{\varepsilon\varepsilon} & \\ & & \end{pmatrix} \begin{pmatrix} \gamma^{(\ell)}_{\varepsilon_1} \\ \gamma^{(\ell)}_{\varepsilon_2} \\ \vdots \end{pmatrix} = \begin{pmatrix} \dot{\gamma}^{(\ell)}_{\varepsilon_1} \\ \dot{\gamma}^{(\ell)}_{\varepsilon_2} \\ \vdots \end{pmatrix} \tag{4}$$

becomes, on transition to the continuum limit,

$$\dot{\gamma}^{(\ell)}_{\varepsilon} = \int d\varepsilon' \rho(\varepsilon')\, D^{(\ell)}_{\varepsilon\varepsilon'}\, \gamma^{(\ell)}_{\varepsilon'} \ , \tag{5}$$

where the $D^{(\ell)}_{\varepsilon\varepsilon'}$ are couplings due solely to the time-derivative operator $\frac{\partial}{\partial t} = \dot{R}\,\frac{\partial}{\partial R}$, i.e., due to motional or nonadiabatic coupling. The diagonal representation pointed to above is then called the adiabatic representation. $\rho(\varepsilon')$ is a suitable density of states. The advantages of this approach are threefold: First, we can get single-channel information for all channels with one equation [compare Eq. (2)]; second, no explicit function relating ε to R need be imposed, as in the Franck-Condon approximation $\varepsilon(R) \approx W_2 - W_1$); third, no truncation of the coupled discretized channels need be used, in fact, discretized channels are not used at all.

$D^{(\ell)}_{\varepsilon\varepsilon'}$ depends explicitly on $\frac{\partial}{\partial t}(W_2 - W_1)$ and $\frac{\partial}{\partial t} V_{\varepsilon}$, and hence on the dynamics. Now two questions arise: What is the potential that one should use for the specification of R(t); and is it channel dependent? Answers: in general, a complex nonlocal potential with dominant part $W_{\varepsilon}(t) = W_1(R) + \frac{\ell(\ell+1)}{R^2} + \varepsilon$; and strictly speaking, yes. The main assumption concerning R(t) we make is that, in the solution for a particular $\gamma^{(\ell)}_{\varepsilon}$, all dynamics is governed by a single trajectory $R_{\varepsilon}(t)$ determined from $W_{\varepsilon}(t)$.

Eq. (5) permits an analytic first-order perturbative solution that reveals clearly the contribution due to the dynamics. Higher-order solutions can in principle be obtained through an iterative procedure but have not been attempted. Even the evaluation of the first-order term can be significantly simplified by the stationary-phase approximation. Thus an integral over t is reduced to a sum over stationary times, further delineating the part played by classical mechanics in this approach. Finally, we point out that if certain approximations are made so that the nonadiabatic couplings $D^{(\ell)}_{\varepsilon\varepsilon'}$ become separable in ε, the differential-integral equation (5) reduces to an integral equation —— a Volterra equation of the second kind —— the exact solutions to which can be much more readily obtained.

B. Multiphoton Resonances in Atom-Atom Scattering

In the realm of radiation-assisted inelastic collisions (RAIC), it has become clear that the exploitation of resonances affords a solution to the problem of achieving good cross-sections at realistic laser intensities[4]. [By "realistic" we mean low enough to be experimentally attainable and also below the intensity threshold required for unwanted side-effects like ionization.] At the same time it has also become apparent that the non-linear and saturation regimes, which have traditionally been thought to require "intense" lasers, can become obvious at much lower intensities.

Laser-induced resonances involve transitions between pairs of electronic states, and attention can therefore be focused on Feshbach rather than orbiting, resonances. Theoretical advances

along these lines have revealed a network of related effects, including transition-state spectroscopy, curve switching and line narrowing. Points of contact have also been established between spectroscopy and laser-induced scattering[4]. In what follows, we shall consider a treatment of laser-induced resonances aimed specifically at the problem of curve switching (in the Landau-Zener sense). The general problem will consist of using a laser, L1, to effect a transition from a particular scattering state to a manifold of bound states. A second laser, L2, is then used to induce multiphoton transitions within this manifold. [In another context, L2 may be regarded as a spectroscopic probe.] Finally, the quasibound intermediate state decays by an emission stimulated by L1 into a different channel (Fig. 1). The reason for including L2 is that it introduces an extra flexibility into the problem and could lead to considerably enhanced probabilities for curve switching, depending on the structure of the potential curves. This illustrates an interesting paradox: in the realm of free-to-free transitions, the introduction of an additional laser reflects a higher-order process associated with a diminution of the cross-section. In the context of resonance scattering, however, another laser can actually enhance the cross-section.

Let us consider the process illustrated in Fig. 1, involving three bound states $|s\rangle$, $|t\rangle$ and $|u\rangle$, and two continua, $|\alpha\rangle$ and $|\beta\rangle$, dressed by two lasers, L1 and L2. In the Breit-Wigner formulation, the T-matrix for curve switching is written as

$$T_{\beta\alpha} = T^{P}_{\beta\alpha} + T^{R}_{\beta\alpha} \quad , \tag{6}$$

where T^P is the potential scattering term, arising from a nonradiative interaction (e.g., spin-orbit coupling), and T^R is the rapidly varying resonant term arising from the radiative interactions with the manifold of bound states. It can be shown that T^R_{fi} can be written as

$$T^R_{\beta\alpha} = \langle \phi^-_\beta | H_{PR}\, \Omega\, H_{RP} | \phi^+_\alpha \rangle \tag{7}$$

where

$$H_{PR} = PHR$$

$$R = \sum_{\nu=s,t,u} |\nu\rangle\langle\nu|$$

$$P = \sum_{\gamma=\alpha,\beta} \int dE' \; |\gamma E'\rangle\langle\gamma E'|$$

α,β is a set of angular momentum quantum numbers describing the open channels in Fig. 1, s,t,u is a set of vibrational and angular momentum quantum numbers describing the three bound states and

$$\Omega = \lim_{\varepsilon\to 0} [E - H_{RR} - H_{RP}(E - H' + i\varepsilon)H_{PR}]^{-1}, \tag{8}$$

where $H' = H_{PP} + H_{PQ}[(1-R)/(E-H_{QQ})]H_{QP}$, $Q = 1-P$.

The matrix Ω^{-1} can be expanded in the basis spanning R, in this case the three bound states $|s\rangle$, $|t\rangle$ and $|u\rangle$. The result is

$$\Omega^{-1} \equiv \begin{pmatrix} \tilde{\Delta}_s + \frac{i}{2}\Gamma_s & V_{st} & 0 \\ V_{st} & \tilde{\Delta}_t + \frac{i}{2}\Gamma_t & V_{tu} \\ 0 & V_{tu} & \tilde{\Delta}_u + \frac{i}{2}\Gamma_u \end{pmatrix} \tag{9}$$

where

$$\Gamma_s = 2\pi \sum_{\gamma=\alpha,\beta} |\langle s|H_{RR}|\gamma\rangle|^2 \qquad (10a)$$

$$V_{st} = \langle s|H_{RR}|t\rangle \qquad (10b)$$

$$\tilde{\Delta}_s = E - E_s - \sum_{\gamma} P \int dE' \frac{|H_{s;\gamma E}|^2}{E - E'} \quad \text{etc.} \qquad (10c)$$

Here, E_s is the energy of the <u>dressed</u> state s.

It remains to determine the in and out scattering states $|\phi_\beta^-\rangle$ and $|\phi_\alpha^+\rangle$ in Eq. (7). Since the matrix elements in (10a) and (10c) are calculated in terms of the standing wave representation of the continuum states, it is economical to use a linear combination of the same states to describe $|\phi_\beta^-\rangle$ and $|\phi_\alpha^+\rangle$:

$$|\phi_\beta^-\rangle = \sum_{\gamma} W_{\beta\gamma} |\gamma\rangle e^{-i\delta_\gamma} \qquad (11)$$

where δ_γ is the phase shift associated with channel γ. The matrix W can then be determined from the S-matrix for potential scattering by

$$S^P_{\beta\alpha} = \sum_{\gamma} W_{\beta\gamma} e^{2i\delta_\gamma} W_{\gamma\alpha} \quad , \qquad (12)$$

i.e., W is the eigenvector matrix of S^P. Eq. (7) can now be written in terms of the W matrix as

$$T^R_{\beta\alpha} = \sum_{\nu\nu'} \sum_{\gamma\gamma'} W_{\beta\gamma} H_{\gamma\nu} Q_{\nu\nu'} H_{\nu'\gamma'} W_{\gamma'\alpha} e^{i(\delta_\gamma + \delta_{\gamma'})} . \qquad (13)$$

In the distorted-wave Born approximation (DWBA) there is a remarkable simplification to Eq. (13) since W is the unit matrix, and T may therefore be written as

$$T_{\beta\alpha} = \left\{ H_{\beta\alpha} + \sum_{\nu,\nu'} H_{\beta\nu}\, \Omega_{\nu\nu'}\, H_{\nu'\alpha} \right\} e^{i(\delta_\alpha + \delta_\beta)} \qquad (14)$$

where $H_{\beta\alpha}$ is the "direct" or potential scattering term. Notice that this involves a definition of T which is $S = 1-2\pi iT$. Another definition common in molecular scattering is $S = 1-iT$, in which the right hand side of (14) would be multiplied by 2π. The factor of $e^{i(\delta_\alpha+\delta_\beta)}$ is of course irrelevant to the calculation of cross-sections, which depend upon $|T|^2$. It may therefore be dropped for convenience. Notice that the DWBA applies only to potential scattering in this case, and aside from this T^R is determined exactly.

To illustrate the possible scattering processes that occur in Fig. 1., we single out three pathways giving rise to curve switching in Fig. 2. The total cross-section for switching from α to β is proportional to $|T_1|^2 + |T_2|^2 + |T_3|^2$, where T_i is the T matrix for process i. The reason that these three pathways are independent is that they give rise to different final state energies. In process 1, energy i is "conserved" so that there is a potential scattering contribution which is missing from processes 2 and 3. The term T^P could arise from spin-orbit coupling and is denoted by the curved arrows in Fig. 2.

The T-matrices can be determined in a consistent way simply by inverting Ω^{-1}. We find:

$$(T_1)_{\beta\alpha} = (T^P)_{\beta\alpha} + \frac{\left(\tilde{\Delta}_t + \frac{i}{2}\Gamma_t\right)\left(\tilde{\Delta}_u + \frac{i}{2}\Gamma_u\right) - V_{tu}^2}{D} H_{\beta s} H_{\alpha s} \qquad (15a)$$

$$(T_2)_{\beta\alpha} = \frac{V_{st}\left(\tilde{\Delta}_u + \frac{i}{2}\Gamma_u\right)}{D} H_{\beta s}H_{\alpha t} \qquad (15b)$$

$$(T_3)_{\beta\alpha} = \frac{V_{tu}\left(\tilde{\Delta}_s + \frac{i}{2}\Gamma_s\right)}{D} H_{\beta t}H_{\alpha u} \qquad (15c)$$

where

$$D = \left(\Delta_s+\tfrac{i}{2}\Gamma_s\right)\left[\left(\tilde{\Delta}_t+\tfrac{i}{2}\Gamma_t\right)\left(\tilde{\Delta}_u+\tfrac{i}{2}\Gamma_u\right)-V_{tu}^2\right]- V_{st}\left(\tilde{\Delta}_t+\tfrac{i}{2}\Gamma_t\right). \qquad (15d)$$

Notice that in each of these terms the effect of <u>all</u> the possible ancillary absorptions and emissions (indicated by the dotted arrows in Fig. 2) are implicitly taken into account. It is clear from (15) that as the energy defects, Δ, of the dressed states approach zero, the resonance states can have a pronounced effect on the magnitude of the cross-section. [The energy defect in this context is essentially the detuning of L2 from exact resonance.] What is particularly interesting is that T_3 has the same order of magnitude as T_1 even though it is a four-photon process! It is possible that under the appropriate circumstances, T_3 might greatly exceed T_1 and T_2. Thus, the introduction of L_2 introduces greater flexibility into RAIC and can be used to drive processes which are not possible with a single laser.

It is worthwhile mentioning the advantages of a formal approach to resonance scattering, as opposed to a coupled-channels procedure. First, the radial portions of the wave functions used to calculate the matrix elements of (15) are independent of the total angular momentum J. This means that the angular momentum couplings can be performed algebraically. In the coupled-channels procedure, the

entire scattering wave function is propagated at once, so that blocks of different J are coupled together. For process 3 in Fig. 2, for example, nine J blocks would be coupled, and obviously this would make a coupled-channels calculation both complicated and time consuming. Second, for a realistic scattering experiment there will always be a distribution of collision energies which must be averaged over to give the observed cross-section. To do this numerically, with a separate calculation at each collision energy, would clearly render a coupled-channels calculation practically impossible.

Finally, we note that the effects of line narrowing [5], previously discussed in reference to photo-ionization, are also evident in the context of laser-induced resonance scattering. This effect arises from the interaction between (or "overlapping" of) closely-spaced bound states and results in a narrowing of the peak in the scattering spectrum, instead of the broadening which would otherwise be expected because of the interaction between the states.

III. Surface Processes: Transitions to Surface States of Semiconductors

For a finite semiconductor, the energy levels are divided into valence, conduction and surface bands [6]. Electrons in valence or conduction states are delocalized throughout the solid. The surface states, however, are confined to the vicinity of the surface. Consequently, this suggests the use of a laser to excite electrons from the valence band into surface states in order to increase the charge in the surface region. This charge can provide a strong Coulombic interaction with an adspecies.

Within a simple one-dimensional model and the nearly-free-electron approximation, we[7] have calculated the energy levels of silicon which are given in Fig. 3. The valence band (V) is occupied in the ground state whereas the conduction band (C) and the surface band (S) are empty. The wave functions associated with the valence states are represented by a sum of plane waves with crystal momentum k, whereas the surface-state wave functions are damped oscillators with crystal momentum $g/2 + i\kappa$. The probability of a transition from the valence state to a surface state is given by

$$M = |\langle \kappa | \vec{A} \cdot \vec{P} | k \rangle|^2, \tag{16}$$

where $\vec{A}$ is the vector potential of the laser radiation and $\vec{P}$ is the momentum operator of the electron. Using the wave functions in this expression, we note that transitions that conserve the real crystal momentum are favored. Consequently, we can write

$$M^2 \approx \frac{(2\pi)^2 \, I \, e^{i\omega t}}{137 \, a \, \omega} \, \delta\left(k - \frac{g}{2}\right) \frac{\left| \left\langle \kappa \left| \frac{d}{dz} \right| \frac{g}{2} \right\rangle_0 \right|^2}{1 - e^{2\kappa a}} \tag{17}$$

where I and ω are the intensity and angular frequency of the laser radiation, the subscript "0" indicates integration over the first unit cell and z is the coordinate along the crystal axis. To first order, the absorption cross-section, σ, can now be written as

$$\sigma = \left(\frac{\omega}{I}\right)\left(\frac{4qL}{V}\right)\int_0^g dk \int_0^{-V/g} d\kappa \; M^2 \; \delta\left(E(\kappa) - E\left(\frac{g}{2}\right) - \omega\right). \tag{18}$$

Here, V is the matrix element of the crystal potential and g the reciprocal lattice vector. We have evaluated this expression for silicon and the results are depicted in Fig. 4. Near the mode in the figure, $|\kappa|$ is greatest and, consequently, the surface density is the greatest. Since the cross-section near this node is quite appreciable, the possibility of using a laser to shift charge from the bulk crystal into the surface region is favorable.

If we now look back at our system before exposure to the laser, the charge density $n_0(z)$, would be given by [8]

$$n_0(z) = \frac{2L}{\pi^2} \int_0^{k_F} dk \left[E_F - E(k)\right] \left|\phi_k(z)\right|^2 , \tag{19}$$

where $\phi_k(z)$ is the valence wave function and E_F is the Fermi energy with wave vector k_F. However, with the laser exciting a surface state the charge density, n(z), would become

$$n(z) = n_0(z) + |\phi_\kappa(z)|^2 \tag{20}$$

where $\phi_\kappa(z)$ is the surface wave function. Since the bulk state that is being excited is delocalized throughout the semiconductor, to be exact we would have to remove an infintesimal amount of charge on the right side of the equation. Eqs. (19) and (20) have been solved, and the results for a typical surface state [$\kappa = -.5|2V/g|$] are presented in Fig. 5. The dramatic increase in surface charge (dashed line) over the ground state charge (solid line) produced by the laser excitation is clearly indicated.

If a charge adspecies were in the vicinity of this surface, the classical change in the interaction potential produced by this excited surface state would be

$$S_{U(z_I)} = \frac{2\pi Z}{\lambda} \int_{-\infty}^{\infty} dz \quad |\phi_\kappa(z)|^2 \; e^{-\lambda|z - z_I|} \tag{21}$$

where Z is the valence of the adspecies at position z_I and λ is the Thomas-Fermi screening parameter [9]:

$$\lambda^2 = \frac{6\pi\bar{n}}{E_F} \tag{22}$$

where $\bar{n}$ is the average electron density of the solid. Results of Eq. (21) are depicted for various excited surface states in Fig. 6. Even for the surface states away from the gap center [$\kappa = .1|2V/g|$], we can see that the change in potential is quite large. Furthermore, the decrease in charge above the surface would suggest that the screening parameter, Eq. (22), would be smaller than the bulk value. Consequently, the interaction and its range given here should be considered a lower limit of the true potential.

We have shown that not only is it possible to populate surface states (Fig. 4), but the induced surface charge is substantial (Fig. 5) and the resultant Coulombic interaction can have a large effect on charged adspecies (Fig. 6). Consequently, a laser could be used to enhance adsorption or desorption by controlling the surface charge.

Acknowledgements

This work was supported in part by the National Science Foundation under Grant CHE-8022874, the Air Force Office of Scientific Research under Grant AFOSR-82-0046 and the Office of Naval Research. The United States Government is authorized to reproduce and distribute reprints for governmental purposes notwithstanding any copyright notation hereon. TFG acknowledges the Camille and Henry Dreyfus Foundation for a Teacher-Scholar Award (1975-82).

References

1. T. F. O'Malley, in Advances in Atomic and Molecular Physics, Vol. 7, ed. by D. R. Bates (Academic Press, New York, 1971), pp. 223-249.

2. J. C. Bellum and T. F. George, J. Chem. Phys. 68 (1978) 134.

3. K.-S. Lam, D. K. Bhattacharyya and T. F. George, Phys. Rev. A, submitted.

4. M. Hutchinson and T. F. George, Mol. Phys., in press.

5. F. H. Mies, Phys. Rev. 175 (1968) 164; K. Rzazewski and J. H. Eberly, Phys. Rev. Letts. 47 (1982) 408.

6. S. Lundquist, in Surface Science, Vol. 1 (International Atomic Energy Agency, Vienna, 1975), p. 331-392.

7. W. C. Murphy and T. F. George, Surf. Sci. 114 (1982) 189.

8. W. C. Murphy and T. F. George, unpublished.

9. C. Kittel, Quantum Theory of Solids, (Wiley, New York, 1963), p. 105.

Figure 1. a) Case of two open channels interacting radiatively with a manifold of bound states by means of a laser, L1. Transitions within the manifold are made by a second laser, L2.

b) The same problem in the "dressed" representation. Here, $|n_i\rangle$ is the number state of the Fock representation of laser i.

Figure 2. The various pathways leading to the curve-switching transition $\beta \leftarrow \alpha$. The ancillary absorptions and emissions of photons from L2 are shown as dotted arrows. These indirect pathways give rise to interferences in the overall T-matrix.

Figure 3. Dispersion relationship in complex crystal momentum space ($k+i\kappa$) for a finite linear chain. The valence, surface and conduction bands are labeled V, S and C, respectively.

Figure 4. Absorption cross-section for surface states, σ, in $Å^2$ versus the frequency of the exciting laser radiation.

Figure 5. Electron density distribution at the surface. The solid line represents the ground electronic state, and the dashed line represents the system with the excited surface state $\kappa=-.5|2V/g|$ in the lower branch.

Figure 6. The magnitude of the surface interaction potential (in millihartrees) at various distances from the surface. The solid line represents the system with excited state $\kappa=-|2V/g|$; the dashed line, $\kappa=-.5|2V/g|$; and the dotted line, $\kappa=-.1|2V/g|$, all in the lower energy branch.

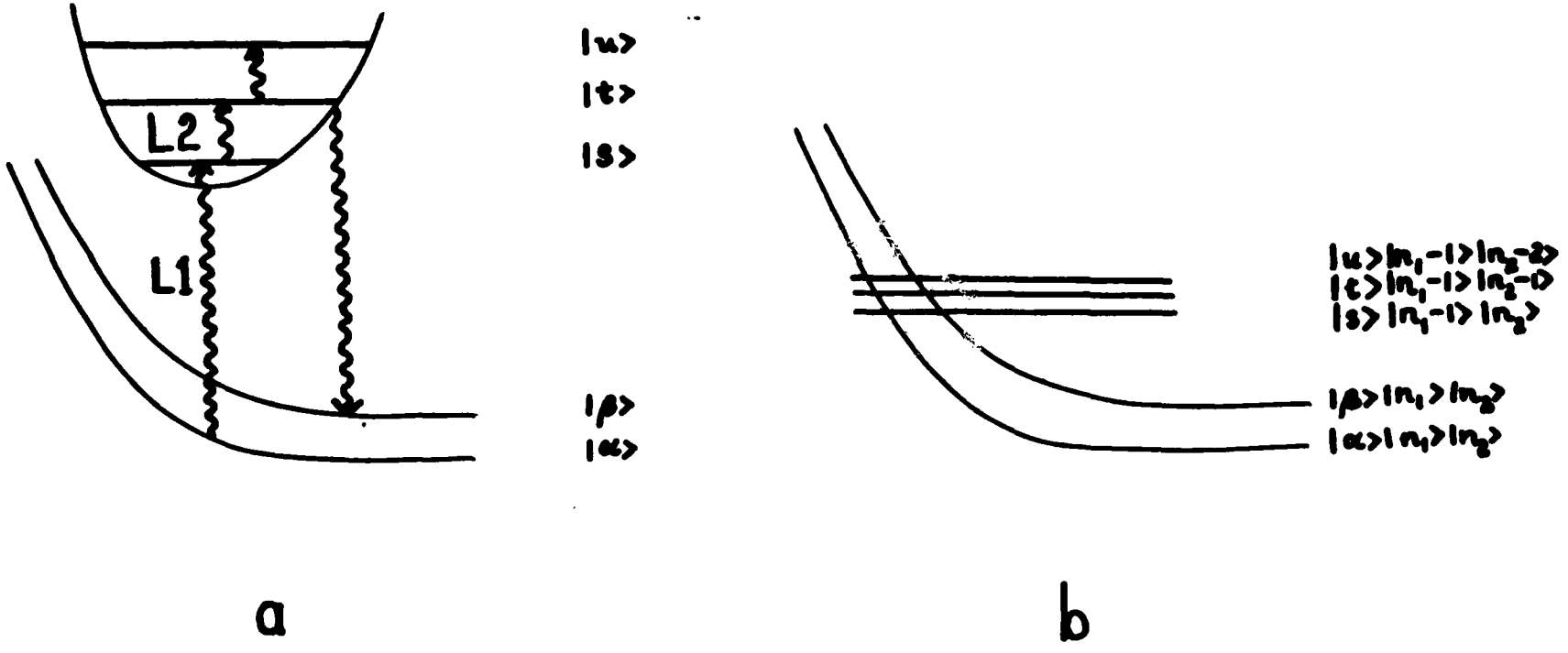

Fig. 1

Fig. 2

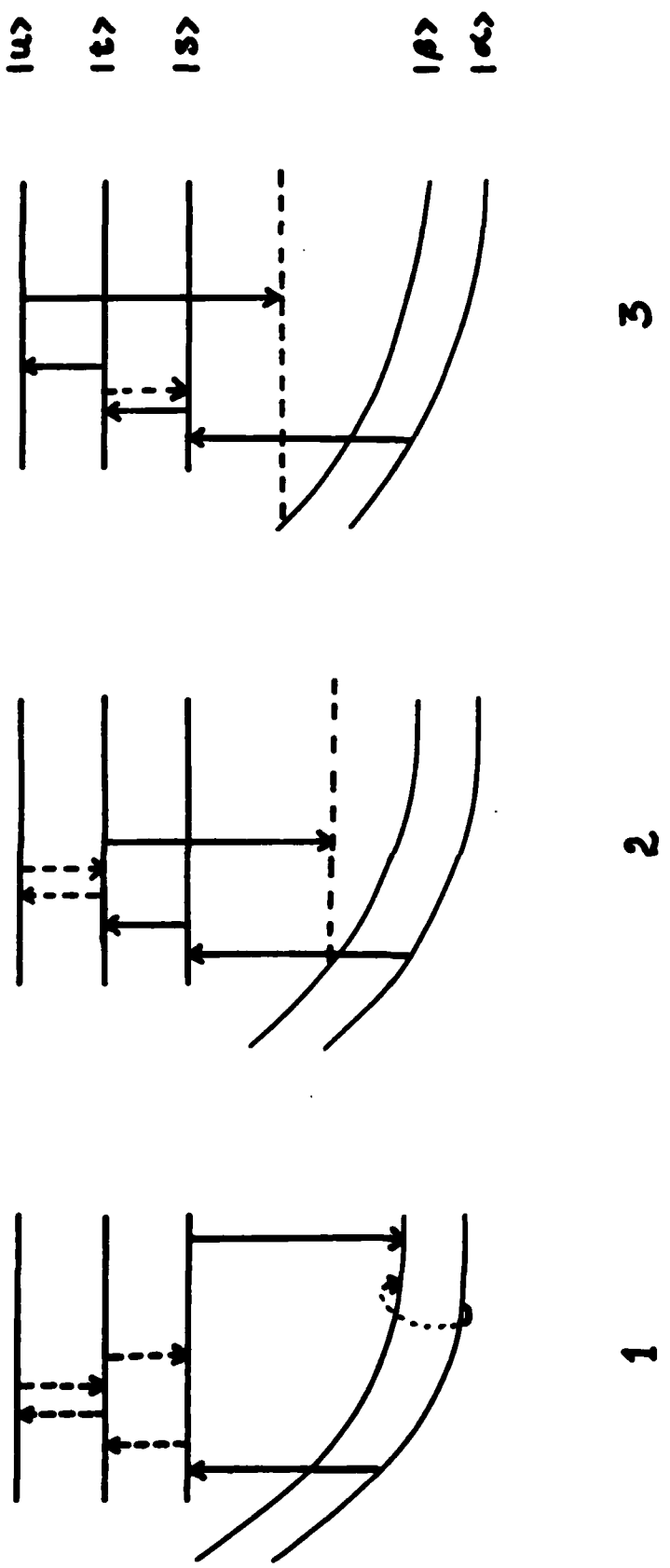

Fig. 3

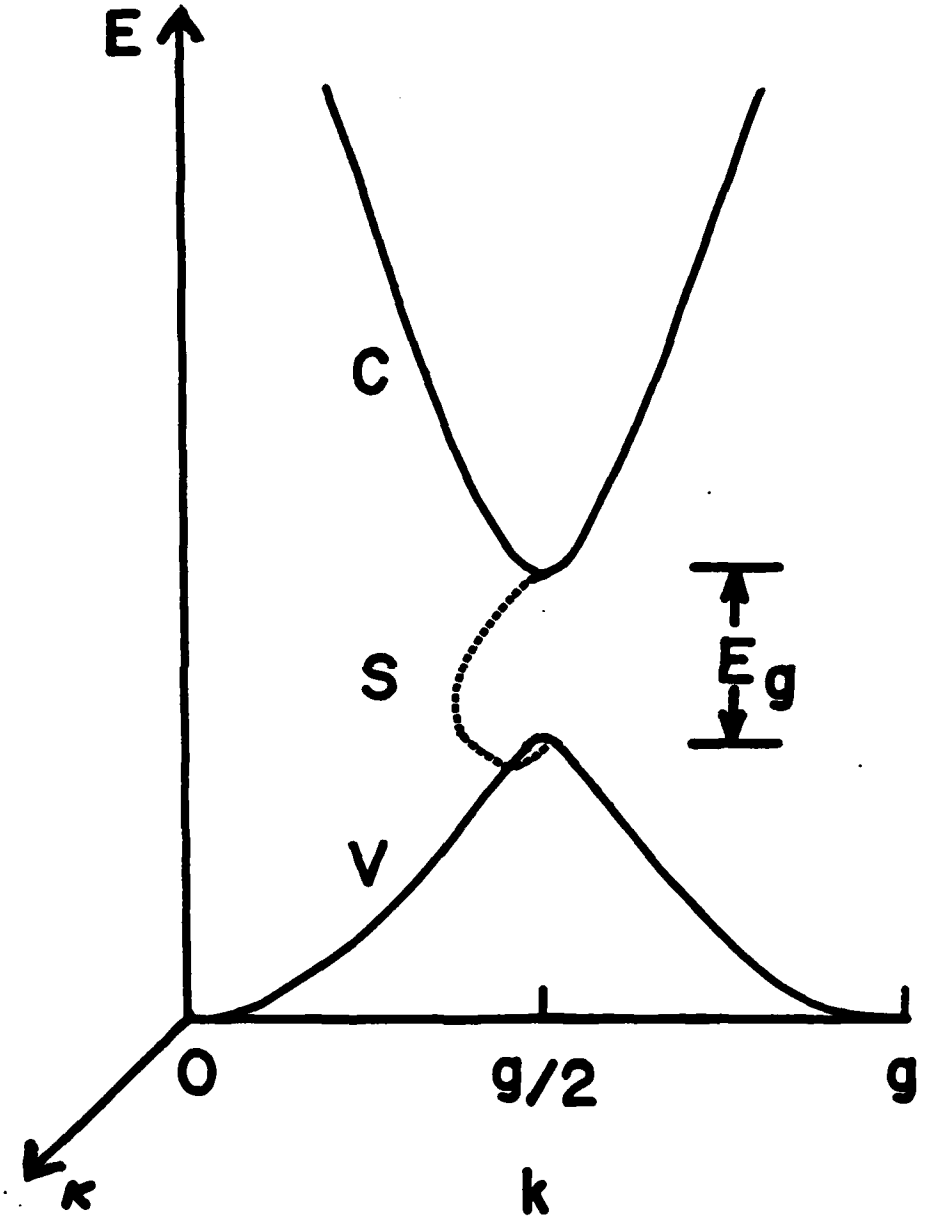

Fig. 4

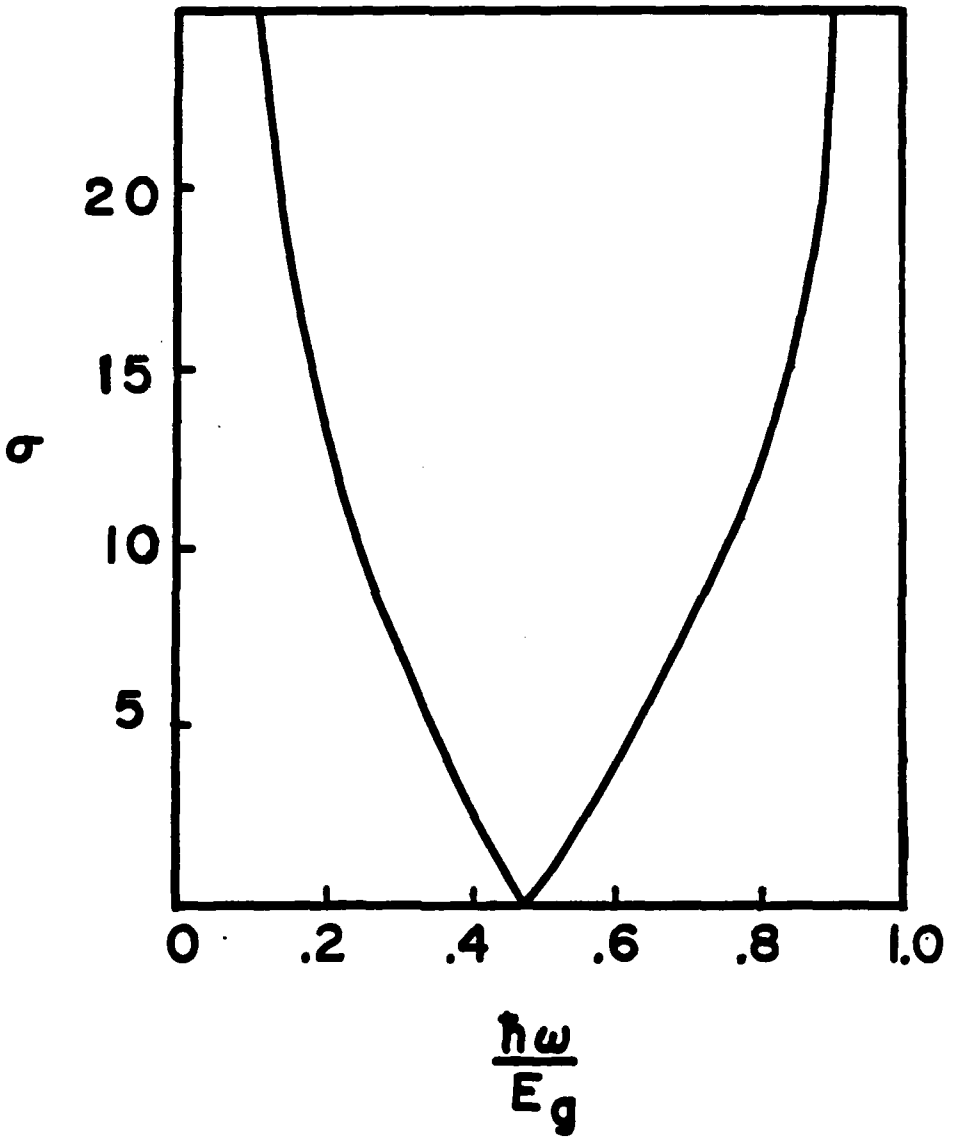

Fig. 5

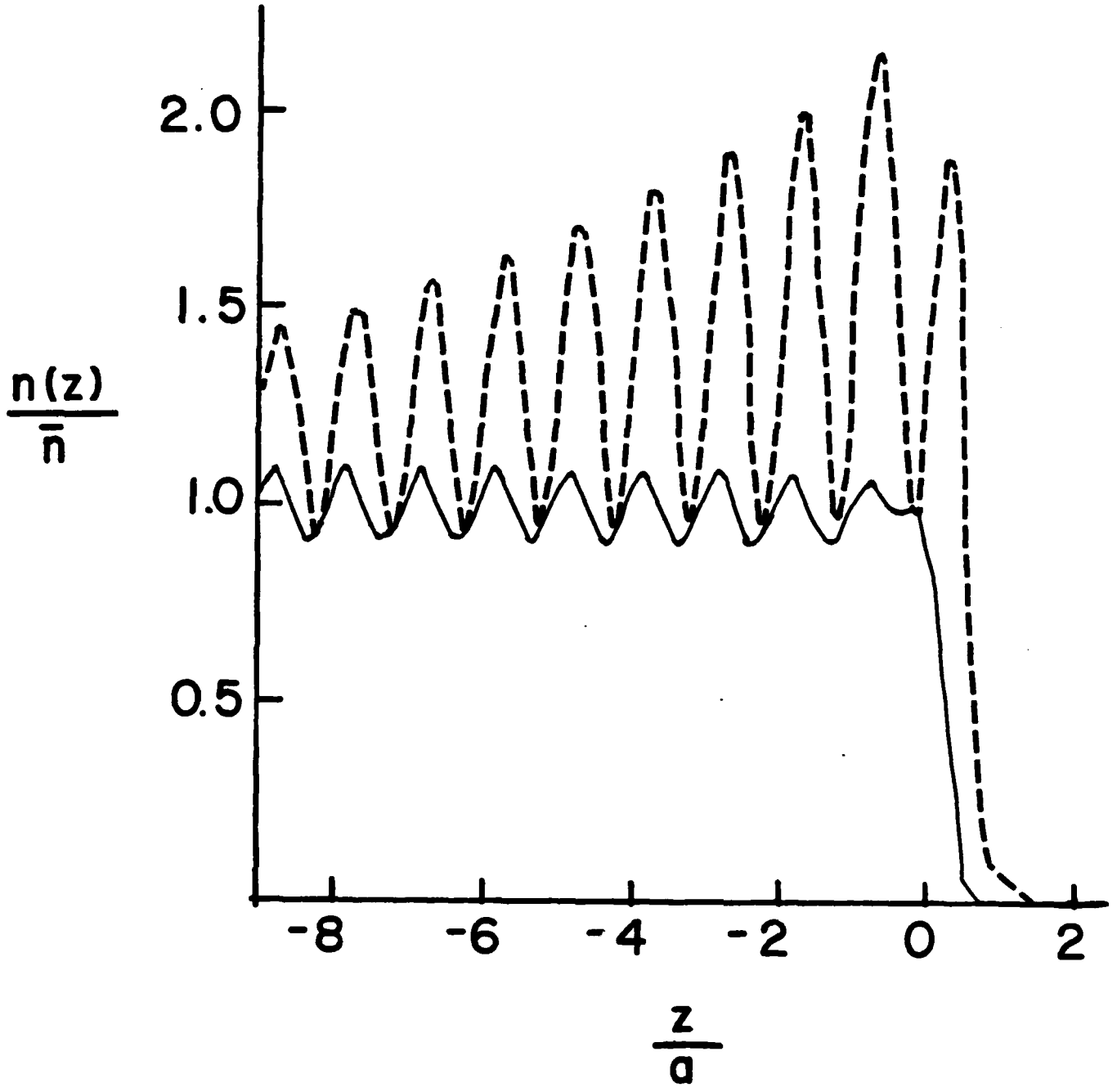

Fig. 6

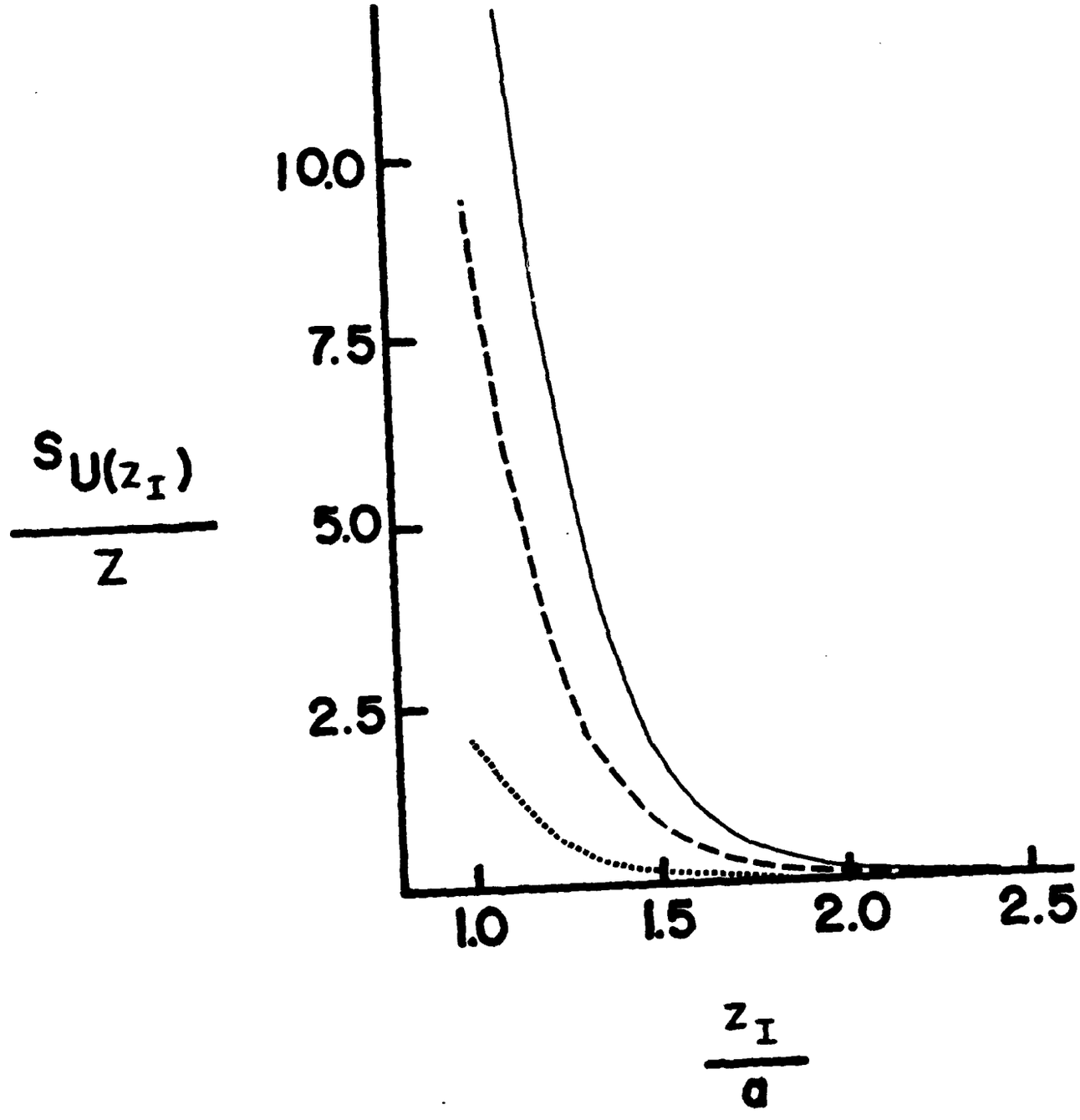

SP472-3/A1

472:GAN:716:enj
78u472-608

TECHNICAL REPORT DISTRIBUTION LIST, GEN

	No. Copies
Office of Naval Research Attn: Code 472 800 North Quincy Street Arlington, Virginia 22217	2
ONR Western Regional Office Attn: Dr. R. J. Marcus 1030 East Green Street Pasadena, California 91106	1
ONR Eastern Regional Office Attn: Dr. L. H. Peebles Building 114, Section D 666 Summer Street Boston, Massachusetts 02210	1
Director, Naval Research Laboratory Attn: Code 6100 Washington, D.C. 20390	1
The Assistant Secretary of the Navy (RE&S) Department of the Navy Room 4E736, Pentagon Washington, D.C. 20350	1
Commander, Naval Air Systems Command Attn: Code 310C (H. Rosenwasser) Department of the Navy Washington, D.C. 20360	1
Defense Technical Information Center Building 5, Cameron Station Alexandria, Virginia 22314	12
Dr. Fred Saalfeld Chemistry Division, Code 6100 Naval Research Laboratory Washington, D.C. 20375	1
Dr. David L. Nelson Chemistry Program Office of Naval Research 800 North Quincy Street Arlington, Virginia 22217	1
U.S. Army Research Office Attn: CRD-AA-IP P.O. Box 12211 Research Triangle Park, N.C. 27709	1
Naval Ocean Systems Center Attn: Mr. Joe McCartney San Diego, California 92152	1
Naval Weapons Center Attn: Dr. A. B. Amster, Chemistry Division China Lake, California 93555	1
Naval Civil Engineering Laboratory Attn: Dr. R. W. Drisko Port Hueneme, California 93401	1
Department of Physics & Chemistry Naval Postgraduate School Monterey, California 93940	1
Scientific Advisor Commandant of the Marine Corps (Code RD-1) Washington, D.C. 20380	1
Naval Ship Research and Development Center Attn: Dr. G. Bosmajian, Applied Chemistry Division Annapolis, Maryland 21401	1
Naval Ocean Systems Center Attn: Dr. S. Yamamoto, Marine Sciences Division San Diego, California 91232	1
Mr. John Boyle Materials Branch Naval Ship Engineering Center Philadelphia, Pennsylvania 19112	1

SP472-3/A17

472:GAN:716:lab
78u472-608

TECHNICAL REPORT DISTRIBUTION LIST, 056

	No. Copies
Dr. G. A. Somorjai Department of Chemistry University of California Berkeley, California 94720	1
Dr. L. N. Jarvis Surface Chemistry Division 4555 Overlook Avenue, S.W. Washington, D.C. 20375	1
Dr. J. B. Hudson Materials Division Rensselaer Polytechnic Institute Troy, New York 12181	1
Dr. John T. Yates Department of Chemistry University of Pittsburgh Pittsburgh, Pennsylvania 15260	1
Dr. Theodore E. Madey Surface Chemistry Section Department of Commerce National Bureau of Standards Washington, D.C. 20234	1
Dr. J. M. White Department of Chemistry University of Texas Austin, Texas 78712	1
Dr. Keith H. Johnson Department of Metallurgy and Materials Science Massachusetts Institute of Technology Cambridge, Massachusetts 02139	1
Dr. J. E. Demuth IBM Corportion Thomas J. Watson Research Center P.O. Box 218 Yorktown Heights, New York 10598	1
Dr. C. P. Flynn Department of Physics University of Illinois Urbana, Illinois 61801	1
Dr. W. Kohn Department of Physics University of California (San Diego) LaJolla, California 92037	1
Dr. R. L. Park Director, Center of Materials Research University of Maryland College Park, Maryland 20742	1
Dr. W. T. Peria Electrical Engineering Department University of Minnesota Minneapolis, Minnesota 55455	1
Dr. Chia-wei Woo Department of Physics Northwestern University Evanston, Illinois 60201	1
Dr. D. C. Mattis Polytechnic Institute of New York 333 Jay Street Brooklyn, New York 11201	1
Dr. Robert M. Hexter Department of Chemistry University of Minnesota Minneapolis, Minnesota 55455	1
Dr. R. P. Van Duyne Chemistry Department Northwestern University Evanston, Illinois 60201	1

TECHNICAL REPORT DISTRIBUTION LIST, 056

	No. Copies
Dr. S. Sibener Department of Chemistry James Franck Institute 5640 Ellis Avenue Chicago, Illinois 60637	1
Dr. M. G. Lagally Department of Metallurgical and Mining Engineering University of Wisconsin Madison, Wisconsin 53706	1
Dr. Robert Gomer Department of Chemistry James Franck Institute 5640 Ellis Avenue Chicago, Illinois 60637	1
Dr. R. G. Wallis Department of Physics University of California, Irvine Irvine, California 92664	1
Dr. D. Ramaker Chemistry Department George Washington University Washington, D.C. 20052	1
Dr. P. Hansma Chemistry Department University of California, Santa Barbara Santa Barbara, California 93106	1
Dr. P. Hendra Chemistry Department Southampton University England SO9JNH	1
Professor P. Skell Chemistry Department Pennsylvania State University University Park, Pennsylvania 16802	1
Dr. J. C. Hemminger Chemistry Department University of California, Irvine Irvine, California 92717	1
Dr. Martin Fleischmann Department of Chemistry Southampton University Southampton SO9 5NH Hampshire, England	1
Dr. J. Osteryoung Chemistry Department State University of New York at Buffalo Buffalo, New York 14214	1
Dr. G. Rubloff I.B.M. Thomas J. Watson Research Center P. O. Box 218 Yorktown Heights, New York 10598	1
Dr. J. A. Gardner Department of Physics Oregon State University Corvallis, Oregon 97331	1
Dr. G. D. Stein Mechanical Engineering Department Northwestern University Evanston, Illinois 60201	1
Dr. K. G. Spears Chemistry Department Northwestern University Evanston, Illinois 60201	1
Dr. R. W. Plummer University of Pennsylvania Department of Physics Philadelphia, Pennsylvania 19104	1
Dr. E. Yeager Department of Chemistry Case Western Reserve University Cleveland, Ohio 41106	2
Professor D. Hercules University of Pittsburgh Chemistry Department Pittsburgh, Pennsylvania 15260	1

TECHNICAL REPORT DISTRIBUTION LIST, 056

	No. Copies
Professor N. Winograd The Pennsylvania State University Department of Chemistry University Park, Pennsylvania 16802	1
Professor F. F. George The University of Rochester Chemistry Department Rochester, New York 14627	1
Professor Dudley R. Herschbach Harvard College Office for Research Contracts 1350 Massachusetts Avenue Cambridge, Massachusetts 02138	1
Professor Horia Metiu University of California, Santa Barbara Chemistry Department Santa Barbara, California 93106	1
Professor A. Steckl Rensselaer Polytechnic Institute Department of Electrical and Systems Engineering Integrated Circuits Laboratories Troy, New York 12181	1
Professor R. D. Archer University of Massachusetts Chemistry Department Amherst, Massachusetts 01003	1
Dr. A. C. Pastor Hughes Research Laboratories 3011 Malibu Canyon Road Malibu, California 90265	1